Muon-induced background for beam neutrinos at the surface

D. Barker[1], E. Church[2], M. Diwan[3], M. Goodman[4], J. De Jong[5], V. A. Kudryavtsev[6], D.-M. Mei[1], M. Richardson[6], M. Robinson[6], K. Scholberg[7], R. Svoboda[8], C. Zhang[1]

[1]*Department of Physics, University of South Dakota, Vermillion, SD 57069, USA*
[2]*Department of Physics, Yale University and FERMILAB, USA*
[3]*Brookhaven National Laboratory, USA*
[4]*Argonne National Laboratory, USA*
[5]*Department of Physics, Oxford University, Oxford, UK*
[6]*Department of Physics and Astronomy, University of Sheffield, Sheffield S3 7RH, UK*
[7]*Department of Physics, Duke University, USA*
[8]*Department of Physics, University of California, Davis, USA*

Abstract

The first simulations of muons at the surface of the Earth have been carried out to characterize and quantify the background from cosmic-ray muons in a liquid argon detector located close to the Earth surface at a depth of about 3-4 metres of rock. We have concentrated on photon-induced cascades as the major source of background events, as we believe this to be the most serious problem. A photon event that converts far from a muon track can be mis-identified as a ν_e interaction, and with limited timing capabilities it is not possible to veto all events with an identified muon. Using GEANT to simulate such muon-induced showering events, a number of possible cuts were devised to suppress this background without inducing large inefficiencies or biases in the ν_e signal. Examples of such cuts are: (1) the angle with respect to the beam, (2) the angle with respect to the incoming muon, (3) the distance to the muon track and (4) the point of closest approach to the muon track. It was found that a combination of cuts on these parameters together with the expected (2%) probability of e/γ misidentification can reject this background down to a few events per calendar year. For events, when a muon does not cross the detector, the fiducial volume cuts in the current nominal design (30 cm from external surfaces, extended to 150 cm from the outgoing beam side) will remove this type of background event. While these are encouraging initial results, there is still more work to do. Current simulations assume perfect reconstruction of the muon track, and shower direction and energy, which makes the current calculation optimistic. On the other hand, the cuts have not been fully optimized (for example, hadron activity at the vertex as a tag to identify ν interactions has not been used) and it is expected that further work will continue to improve rejection. In addition, the effect of dead regions inside the detector (also with 30 cm fiducial volume cut as in the current design) need to be included and simulation statistics needs to be increased. Due to a very large number of cosmic-ray muons and their secondaries, in particular electrons, other rare background events

mimicking electron neutrino interactions have to be studied with higher statistics.
Exact site parameters also have to be considered. Positioning the detector behind a hill will remove near horizontal muons which are responsible for a large number of background events near parallel to the beam. Additional photon detectors able to observe muon secondaries, will reduce the cosmogenic background below 1 event per year. An active veto system around the detector also needs to be considered although it may not be necessary unless the fiducial volume is extended closer to the detector surfaces.

1 Introduction

The LBNE Working group 'Cosmic Rays and Cosmogenics' was set up at the beginning of 2012 to address cosmic-ray induced background for underground location of the LBNE detector when such a location was considered as a viable option (before the DoE recommendation for a phased approach). As a result of this work (including a large set of simulations completed before the formal creation of the working group) a number of important results were obtained and conclusions reached, the most important ones being:

- Muon generators have been written for different underground locations and evaluation of muon fluxes and energy spectra has been carried out (see, for example LBNE-doc-3144, LBNE-doc-4155, LBNE-doc-5833)
- It was shown that with a soft cut on the fiducial volume of LAr, a proton decay search via the decay mode of $p \to K\bar{\nu}$ can be carried out at shallow depth $\sim$ 800 feet (LBNE-doc-5440, LBNE-doc-5852, LBNE-doc-5851, LBNE-doc-5904).
- The first evaluation of the cosmogenic background for supernova neutrino burst (SNB) search has been completed (arXiv:1202.5000v1 [physics.ins-det], LBNE-doc-5822, LBNE-doc-5909).

Since then it has become apparent that funding constraints may prevent quick construction of the LBNE liquid argon (LAr) detector at the underground location at Homestake. The phased approach recommended by DoE limits the size of the detector to about 10 kt fiducial mass in the first phase and its construction will be carried out on the surface unless additional funding can be found from sources other than DoE.
With a detector located on the surface, it is unlikely that the LBNE experiment will be able to carry out any physics tasks beyond neutrino oscillation study using beam neutrinos from Fermilab. (SNB is still under investigation but will require a sophisticated trigger to not miss a neutrino burst while limiting the amount of data recorded. In addition, spallation backgrounds may be prohibitive). With a relatively slow argon TPC as a target it was not obvious that the detection of beam neutrinos would be unaffected by a large backgrounds generated by cosmic-ray muons. In these circumstances the main objectives of the WG on cosmogenics has shifted to the evaluation of cosmic-ray background for beam neutrinos, primarily ν_e, on the surface. The main problem arises from the long drift time of electrons in the TPC ($\approx$ 1.4 ms), which

is much bigger that duration of the beam spill (≈ 10 μs). This is to be compared with other neutrino detectors on the surface, which typically have readout times of less than a μsec. This note summarizes our first preliminary evaluation of background produced by cosmic-ray muons and their secondaries if an LBNE detector based on liquid argon is located near the surface at a shallow depth of 3-4 meters.

2 Beam parameters and muon fluxes

To sample muon energy and zenith angle on the surface we have used the parameterisation proposed by Gaisser [1], modified to include large zenith angles, fraction of prompt muons and muon decay in the atmosphere:

$$\begin{aligned} \frac{dI_\mu}{dE_\mu d\Omega}(E_\mu,\theta) &= 0.14 \times (E_\mu + \Delta)^{-2.70} \times p_d \\ &\times \left(\frac{1}{1 + \frac{1.1 E_\mu \cos\theta^\star}{115 GeV}} + \frac{0.054}{1 + \frac{1.1 E_\mu \cos\theta^\star}{850 GeV}} + R_c \right), \end{aligned} \quad (1)$$

where $\frac{dI_\mu}{dE_\mu d\Omega}(E_\mu,\theta)$ is the differential muon intensity at sea level in units cm^{-2} s^{-1} sr^{-1} GeV^{-1}, E_μ is the muon energy at the surface in GeV, θ is the muon zenith angle at the surface, $\theta^\star$ is the muon zenith angle at the height of muon production, Δ is the muon energy loss in the atmosphere (important for low-energy muons only), $R_c = 10^{-4}$ is the ratio of prompt (e.g charm decay) muons to pion generated muons, p_d is the probability for a muon to not decay in the atmosphere. There are several parameterisations for the $\cos\theta^\star$ as a function of θ which take into account the curvature of the Earth atmosphere. In some parameterizations correction factor for muon decay is included in the term Δ and then $p_d = 1$ (see [2, 3, 4, 5] and references therein for more details). The total muon flux on the surface of the Earth through a sphere is equal to 170 m^{-2} s^{-1}, whereas a flux through a horizontal plane is 130 m^{-2} s^{-1} [6]. Positioning the detector at a depth of 10 m w. e. underground will reduce the flux on the detector by approximately a factor of 2. If the detector is 3 metres below the ground the expected flux through a sphere will be ~ 100 m^{-2} s^{-1}.

In further evaluation we assume that the beam spill has a duration of 10 μs whereas the maximum drift time within a cell is 1.4 ms. We assume that a 10 kt detector with a size of 30 m (length along the beam) $\times$ 15 m (width) $\times$ 16 m (height) is located on the surface of the Earth at Homestake and is shielded by 3 m of rock with a density of 2.71-2.82 g/cm^3 (the type of shielding is not crucial here as long as the column density does not change). We assume that the shielding is sufficient to absorb electromagnetic and hadronic components of atmospheric air showers leaving only muons as the source of background for beam neutrinos. 3-4 metres of rock will suppress the hadronic component of cosmic rays by at least an order of magnitude. With the muon flux at the detector location of about 100 m^{-2} s^{-1} through a sphere, the muon event rate in the detector is about 70 for 1.4 ms event record. Assuming 1.33 s spill repetition

time and 2×10^7 s of beam running per calendar year, the total duration of the data collection (with 1.4 ms time window per spill) per year is 21053 s. We expect then about 10^9 muons passing through the detector in a calendar year. If an independent trigger for a beam neutrino induced event can be provided (for instance, by the light detector – arrays of PMTs), then the time window for beam data collection can be reduced to 10 μs and the total data collection time and hence, the number of muons, per calendar year can be 140 times less: 150 s and about 7.1×10^7 muons, respectively.

The beam is assumed to be pointing 6° upwards along the long side of the detector and the Earth surface is assumed to be flat. There is an option to position the LBNE detector beyond the hill to suppress the flux of atmospheric muons coming from directions close to the beam. Detailed simulations for this design will be completed later.

3 Muon-induced background

As discussed in LBNE notes [7, 8] the main problems of running the detector on the surface can briefly be summarized as: 1) high event rate for DAQ to handle; 2) high data rate for processing and analysis; 3) track confusion; 4) cosmogenic backgrounds.

After discussing these problems within the cosmogenic group we concluded that:

1. High event rate is unlikely to be a problem. LHC experiments have demonstrated that modern data acquisition systems are capable of processing events separated by tens of nanoseconds. In fact, only about 1.4 ms of data (or slightly more) are needed to be processed (which corresponds to the maximum drift time) every 1.33 s since no physics other than with beam neutrinos is likely to be possible on the surface.

2. Similar considerations apply to the data transfer, online processing and analysis.

3. Track confusion may be a problem but does not look as severe as a "background" problem. As soon as the background problem is better understood and the reconstruction software for specific detector configuration is working, we can consider in more detail the "confusion" problem.

4. Cosmogenic background appears to be the most severe of the aforementioned problems. In this note we will consider cosmogenic background induced by muons and their secondaries.

We believe that the main problem caused by cosmic-ray muons is mimicking the ν_e interaction events. We expect to detect less than 100 ν_e interactions per calendar year in a 10 kt detector and need the cosmogenic background to be much smaller than this event rate. We assume that the signal events of interest will be in the energy range of 0.5-5 GeV. Note that this corresponds to a neutrino energy. Since in charge-current neutrino interactions not all neutrino/antineutrino energy is transferred to an electron/positron, the energy of electron-induced cascade can be smaller than the minimum neutrino energy of 0.5 GeV, with part of neutrino energy being transferred to hadrons.

Below is the list of some potential sources of background (also discussed in [9]), possible ways to mitigate them and potential loss of effective volume:

- *Electron tracks, e^+e^- pairs or tracks of any other charged particle produced by a muon or any other charged particle in a cascade.* The vast majority of these events will be associated with knock-on electron and e^+e^- pair production by muons. Rejecting this background is relatively easy: we will need to cut a cylinder of a few cm diameter around a muon track and any charged secondary track, requiring a candidate neutrino event to start outside such a cylinder. This will remove all charged tracks associated with a muon and other charged particles with a loss of about 1% of fiducial volume. Some of the tracks may start in, end in or pass through the dead regions. This will require removing volumes (a few cm thick) close to dead regions. This is probably needed to be done anyway since ν_e interactions in dead regions may not provide enough information about the energy of the event. Similar cuts should be applied to the surface of the detector (charged tracks entering the detector should not be considered as candidate ν_e interactions). In total the fiducial volume could be as much as 90% of the total volume. The fiducial volume cut will also help to avoid track confusion. It is worth noting that the current design includes 30 cm cut around dead regions and detector surfaces.

- *Bremsstrahlung from muons.* As we require a photon to have an energy more than 0.5 GeV, the probability of emitting such a photon at a large angle from the muon track is quite small. Photons (and induced electromagnetic cascades) travelling close to the original muon can be rejected in the same way as charged tracks.

- *Neutral hadrons.* Among these hadrons, the most dangerous are π^0 giving two photons, K^0_S decaying into two neutral pions and then 4 photons, and neutrons giving neutral pions and again photons. In all these cases we will have two or more photons in the final stage.

- K^0_L *decay.* This is in fact a special case of neutral hadron production and decay which can mimic ν_e interactions. The signature of the decay can be exactly the same as the signature of the signal event. K^0_L can decay into $\pi^\pm$, $e^\mp$ and $\bar{\nu}_e/\nu_e$. In most cases K^0_L will decay at rest (losing energy in hadronic interactions before it decays) and the kinetic energy of the electron will be significantly below the minimum energy of interest – 0.5 GeV. However, since the energy of an electron from a neutrino interaction can also be smaller than 0.5 GeV if part of the energy is transferred to the produced pion, there is a danger that a K^0_L decay in some cases can be indistinguishable from a neutrino event. The total number of K^0_L above 0.5 GeV in the detector will be about 1500 per calendar year but first simulations indicate that less than 10% of them produce electrons (via decay) with energy above 0.1 GeV. Due to the kaon rest mass, no events would have an electron energy greater than 0.5 GeV.

Due to a very limited time available so far for the study of the background, we present here the status of the investigations which have been focused on three important issues:

1. The rate of background events from muons which cross the detector and different cuts and selections which can decrease it.

2. The efficiency of the Point of Closest Approach (PoCA) technique to remove electron tracks which can point back to a muon or another charged track in a muon-induced cascade.

3. The rate of background events caused by muons which did not pass through LAr and ways to suppress this background.

4 Background events caused by muons passing through the detector

The performance of the LBNE LAr detector and analysis in rejecting background events depends crucially on the accuracy of the neutrino energy and angle reconstruction. Figure 1 [10] shows the simulated distribution of electron angle w.r.t. the beam as a function of the electron energy for events induced by neutrinos. Above 0.5 GeV most events lie within a 40° angle w.r.t. the beam (θ_b). Hence rejecting events with θ_b greater than 40° would remove most of the background, at the same time keeping most of the signal events. A significant fraction of background events "near parallel" to the beam is produced by muons moving close to the horizon. Hence, placing the detector beyond the hill will help reducing this background also. Such a hill indeed exists at the candidate surface site at Homestake.

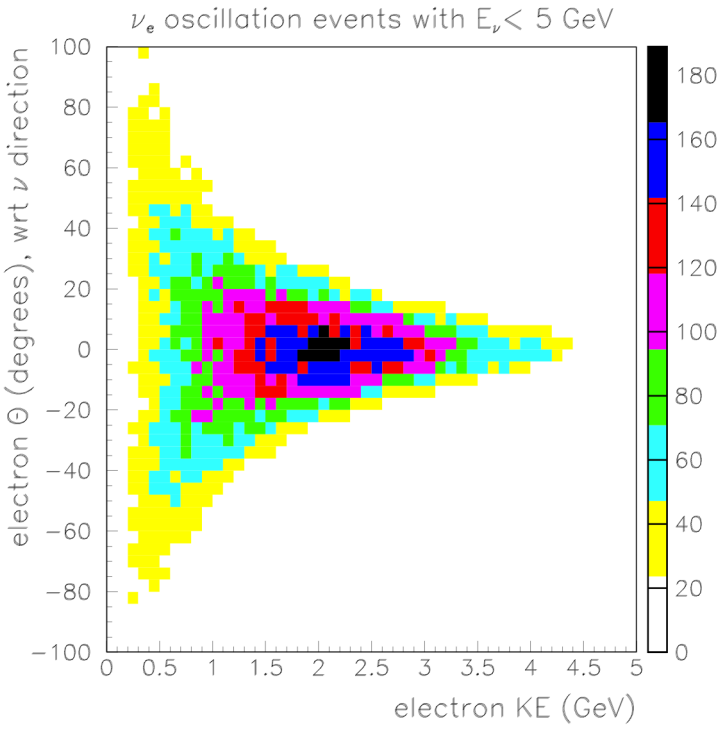

Figure 1: Projected electron emission angle as a function of electron energy in electron neutrino induced events [10].

At energies below 1 GeV, a non-negligible number of signal events have θ_b greater than 40° and rejecting background events based on this cut by itself is not efficient. In this study we concentrated mainly on the following events and parameters (see [12] for details):

- We have assumed that the vast majority of events mimicking electromagnetic cascades induced by electron neutrinos should be due to similar cascades induced by photons. (We have not studied in detail yet a potential background caused by K_L^0 decay, but the rate of decays with high energy electrons is quite small due to the kaon rest mass.) Photons can be produced by any other particles also, but the final state particle should be the photon to produce e^+e^--pair and then electromagnetic cascade.

- We have recorded photons and their parameters at the locations where they convert into e^+e^--pairs. The resulting cascades should point to the initial photons.

- We have recorded the photon energy, E_{ph}, and calculated the angle of each photon from the beam direction, θ_b, the angle from the muon track (assuming the muon track is a straight line), θ_μ, and the distance from the muon track, d. We have counted individual photons and if two photons were produced in π^0 decay, they were counted as two separate events rather than one. Estimates show that this may overestimate the background event rate by up to 20%. Similarly, for high-energy electromagnetic cascades with several photons, each photon was counted as a separate event. This again overestimates the number of events although technically, cascades from individual photons may still mimic neutrino induced cascades.

Table 1: The number of photons per calendar year produced in a 10 kt liquid argon detector on the surface (no cut on initial muon energy). Photons with energies between 0.5 GeV and 5 GeV were selected. Different rows show events with different cuts on the angle with respect to the muon, θ_μ, and columns show events with different cuts on the distance from the muon track, d.

Cuts on d θ_μ	> 0 cm	> 10 cm	> 20 cm	> 30 cm	> 50 cm
$> 0°$	1.02×10^8	4.19×10^6	1.33×10^6	6.05×10^5	2.33×10^5
$> 2°$	1.36×10^7	1.13×10^6	5.14×10^5	2.92×10^5	1.35×10^5
$> 3°$	4.98×10^6	1.67×10^6	6.74×10^5	3.61×10^5	1.51×10^5
$> 5°$	2.53×10^6	7.57×10^5	3.74×10^5	2.25×10^5	1.09×10^5
$> 10°$	1.53×10^6	5.00×10^5	2.62×10^5	1.60×10^5	7.90×10^4

We have simulated 50 million muons with energy ≥ 1 GeV passing through a cylinder (40 m diameter and 19 m height) which encompasses the LAr detector. (Although muons were sampled on a surface of a cylinder, their tracks were extrapolated backwards to the surface of the Earth and then these muons were transported using GEANT4 through the rock around the detector.) The muon flux ($E \geq 1$ GeV) through the cylinder without taking into account the muon absorption is 2.82×10^5 s^{-1}. This gives the normalisation to the simulations. 5×10^7

Table 2: The number of photons per calendar year produced in a 10 kt liquid argon detector on the surface by muons having an energy on the surface more than 10 GeV. Photons with energies between 0.5 GeV and 5 GeV were selected. Different rows show events with different cuts on the angle with respect to the muon, θ_μ, and w.r.t. the beam, θ_b. Different columns show events with different cuts on the distance from the muon track, d.

Cut on d	> 0 cm	> 10 cm	> 20 cm	> 30 cm	> 50 cm
$\theta_\mu > 0°$	9.85×10^7	3.03×10^6	9.22×10^5	4.60×10^5	1.64×10^5
$\theta_\mu > 0°$, $\theta_b < 40°$	3.93×10^6	1.89×10^5	7.25×10^4	3.76×10^4	1.01×10^4
$\theta_\mu > 2°$	1.21×10^7	1.11×10^6	4.28×10^5	2.34×10^5	1.07×10^5
$\theta_\mu > 2°$, $\theta_b < 40°$	4.50×10^5	6.33×10^4	3.00×10^4	1.73×10^4	8.69×10^3
$\theta_\mu > 3°$	4.17×10^6	7.61×10^5	3.28×10^5	1.86×10^5	8.64×10^5
$\theta_\mu > 3°$, $\theta_b < 40°$	1.90×10^5	4.27×10^4	2.25×10^4	1.37×10^4	7.68×10^3
$\theta_\mu > 5°$	2.18×10^6	5.66×10^5	2.61×10^5	1.48×10^5	7.10×10^4
$\theta_\mu > 5°$, $\theta_b < 40°$	1.23×10^5	3.29×10^4	1.83×10^4	1.13×10^4	6.68×10^3
$\theta_\mu > 10°$	1.40×10^6	4.10×10^5	2.01×10^5	1.17×10^5	5.76×10^4
$\theta_\mu > 10°$, $\theta_b < 40°$	9.25×10^4	2.56×10^4	1.49×10^4	9.47×10^3	5.61×10^3

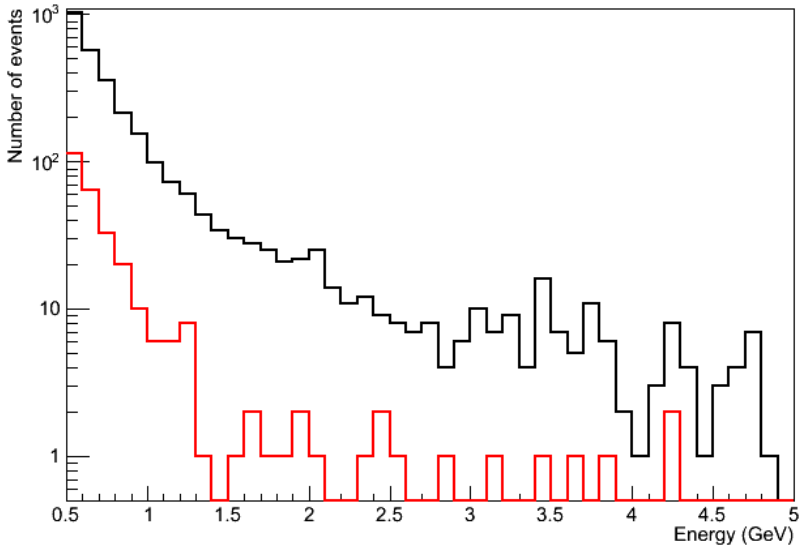

Figure 2: Energy spectra of photons at $d > 50$ cm from muon tracks and an angle $\theta_\mu > 5°$ w.r.t. the muon. Initial muons have energies more than 10 GeV on the surface. Black histogram shows the spectrum for all photons, red histogram – only for photons with $\theta_b < 40°$.

simulated muons correspond to 177 s of live time which is $177/21053 = 0.00842$ of calendar year of beam running. The results of the simulations are summarized in Table 1 which shows the number of background events per year. There is no cut on θ_b, but the results of cuts on d and θ_μ are shown. The lowest statistics in the last column correspond to approximately a

few tens of detected events. Note that only photons with energies between 0.5 GeV and 5 GeV have been selected. Extension to photon energies down to 0.1 GeV is underway and will be included in future reports.

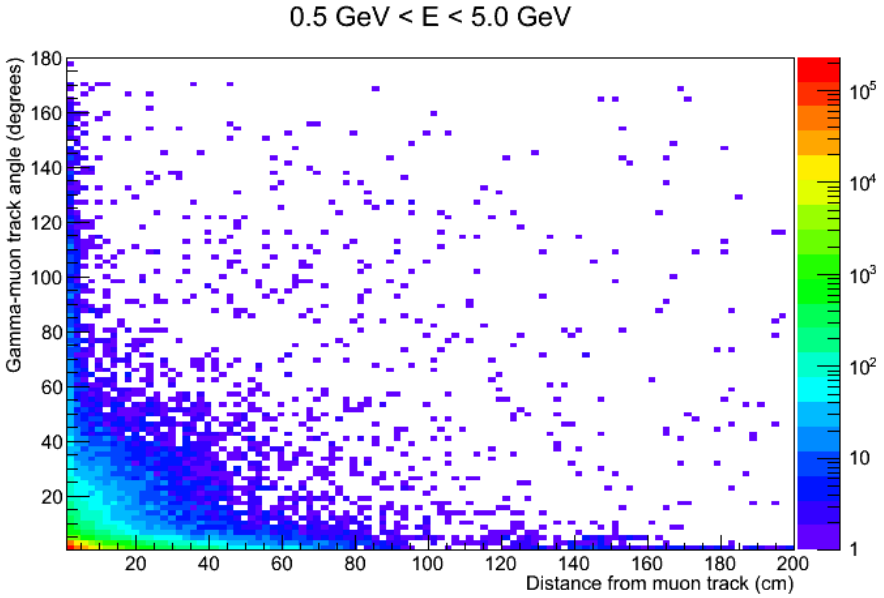

Figure 3: Photon angles w.r.t. the muon tracks, θ_μ, versus distances from the muon tracks, d, for 0.5-5 GeV photons. Initial muons have energies more than 10 GeV on the surface.

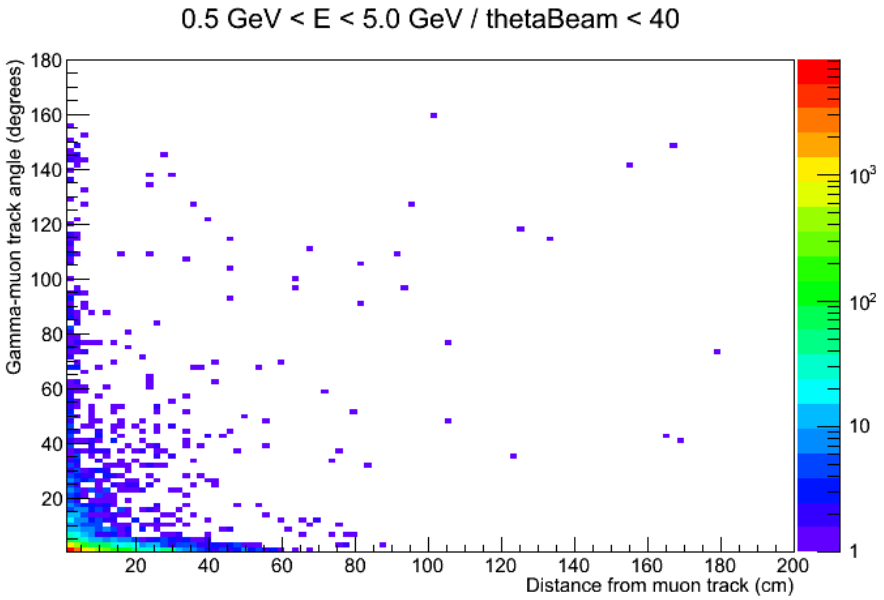

Figure 4: Photon angles w.r.t. the muon tracks, θ_μ, versus distances from the muon tracks, d, for 0.5-5 GeV photons having the angle w.r.t. the beam $\theta_b < 40°$.

Since much larger statistics are required to characterize the background with better precision, we have completed another simulation run propagating 50 million muons with energy ≥ 10 GeV, under the assumption that they are potentially more capable of producing background events. In this case the statistics corresponded to 0.0419 calendar years. Table 2 gives background event rates from muons with $E \geq 10$ GeV with similar cuts on d and θ_μ. In addition, a "soft" θ_b cut of 40° is also made for comparison with the "no cut" rate. Comparing Tables 1 (photons from all muons) and 2 (photons from muons with $E > 10$ GeV), we can see that most background photons (from 65% at large distances from a muon track up to almost 100% at small distances) are produced by high-energy muons. We can conclude that the approach of simulating primarily high-energy muons ($E \geq 10$ GeV) is justified although we underestimate the background rate with certain cuts by up to 35%. Figures in this Section show plots of the characteristics of photons produced by 50 million muons with energies greater than 10 GeV.

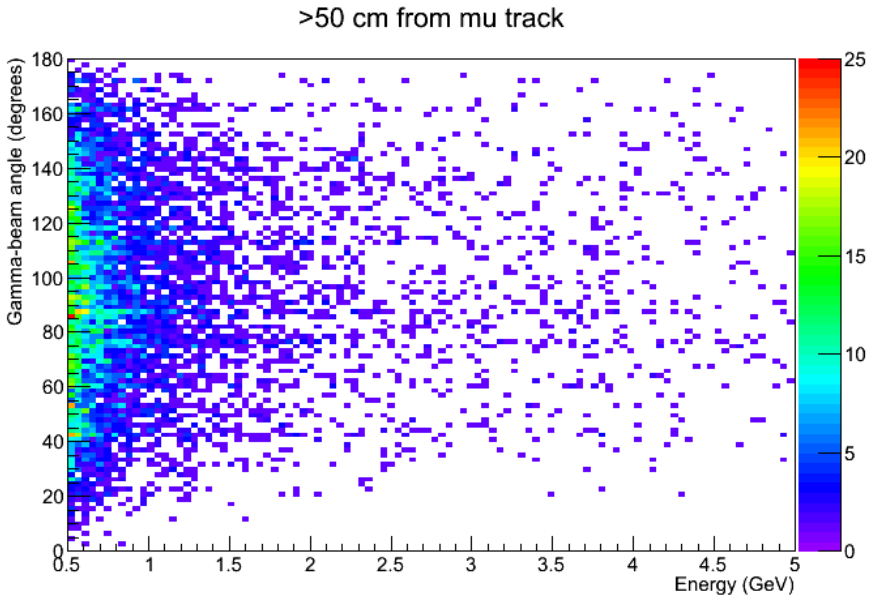

Figure 5: Photon angles w.r.t. the beam, θ_b, versus photon energy for photons with distances from muon tracks greater than 50 cm. Initial muons have energies more than 10 GeV on the surface.

If a soft cut of $\theta_b < 40°$ is made on background events, along with cuts of $\theta_\mu > 10°$ and $d > 50$ cm to the parent muon, then a background rate of 5610 events per year is obtained. Correction for events produced by muons with $E_\mu < 10$ GeV is required but has not been done here. Additional rejection of photon-induced cascades (98% efficient [13]) via analysis of the event vertex (i.e. using the e/γ separation capability of the TPC) reduces this rate to 112 per calendar year. Tracking a cascade back to the muon track (not always possible since a photon may not be produced by the muon) or other particles in a cascade, offers additional rejection capabilities. Note also that this rate is negligible < 1 event per year if we assume that the 10 μs beam spill window can be used instead of the drift time, which might be possible with an efficient photon detector and/or fast veto.

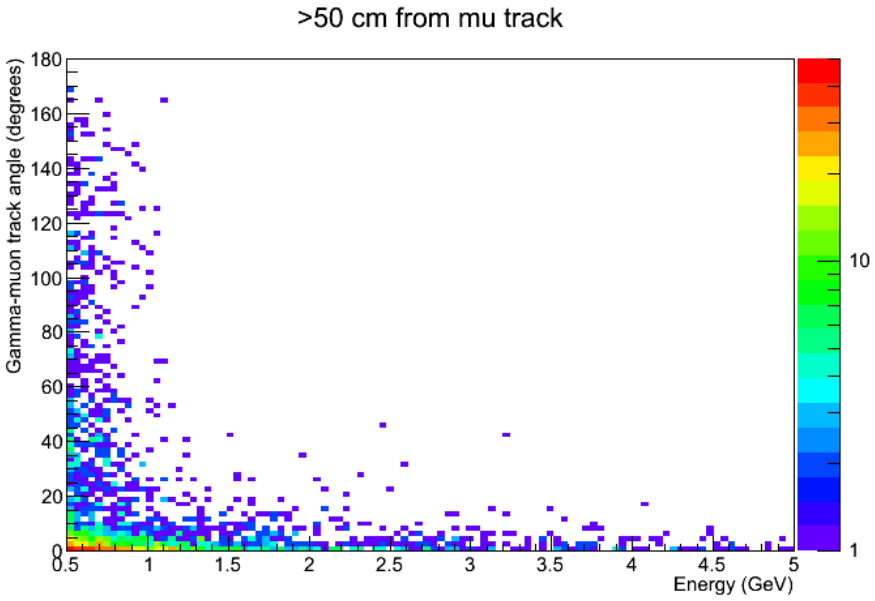

Figure 6: Photon angles w.r.t. muons, θ_μ, versus photon energy for photons with distances from muon tracks greater than 50 cm. Initial muons have energies more than 10 GeV on the surface.

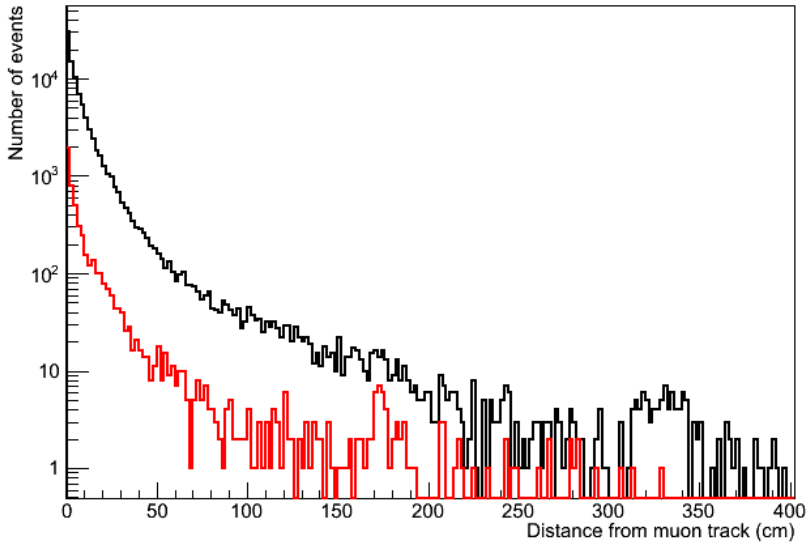

Figure 7: Distribution of distances from muon tracks for photons with angles w.r.t. muons $\theta_\mu > 5°$. Initial muons have energies more than 10 GeV on the surface. Black histogram shows the distribution for all photons, red histogram – only for photons with $\theta_b < 40°$.

Low-energy photons are more numerous (Figure 2) and more dangerous (Figure 6) compared

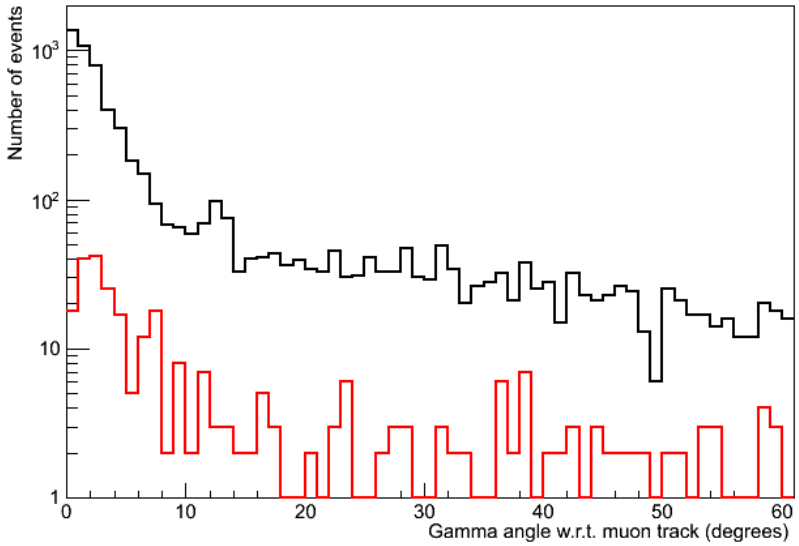

Figure 8: Distribution of photon angles w.r.t. muons for photon distances greater than 50 cm from the muon tracks. Initial muons have energies more than 10 GeV on the surface. Black histogram shows the distribution for all photons, red histogram – only for photons with $\theta_b < 40°$.

to high-energy ones. The spread of angles and distances w.r.t. muon tracks is much larger for low-energy photons. The background from muons passing through the detector is more serious at low energies, where θ_b cuts begin to affect signal efficiency. Thus we have also investigated more sophisticated cuts, such as one based on the Point of Closest Approach (PoCA). This is discussed in the next section.

5 Rejecting background events using point of closest approach technique

Although the absolute event time of a muon will not be known without a high efficiency photon detector, the time between a muon and secondary can be assumed to be much less than the characteristic drift time of ~ 1 ms, allowing a relative fit between the muon track and shower vertex and direction. Ideally, the shower track will project back to the muon track allowing it to be identified as a secondary muon event. In practice, there will be uncertainty in both the shower and muon tracks, and thus the Point of Closest Approach (PoCA) is the relevant quantity that is used. This section describes an independent simulation and analysis to investigate this technique.

In this set of simulations the detector was positioned in a pit (see [15] for details). The schematic of the detector and overburden put into GEANT4 is shown in figure 9. The top of the detector is parallel with the surface, with the rest of the detector being below grade. A 3 m gap was

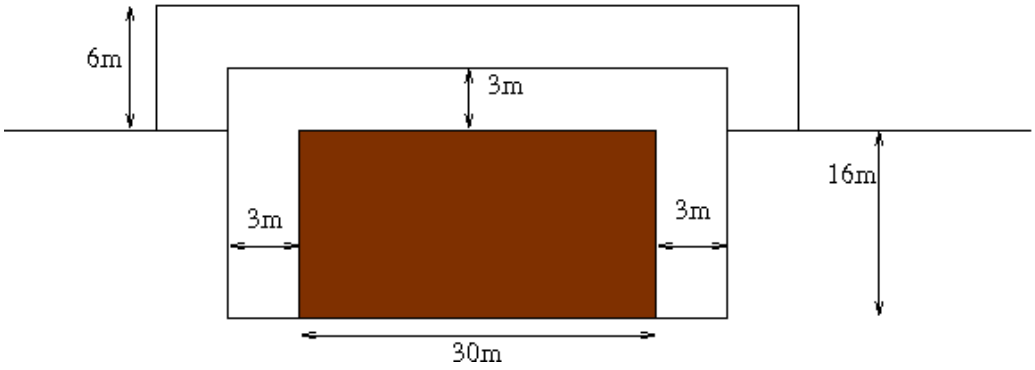

Figure 9: The simulated 10 kt liquid argon detector with a size of 30 m (length) × 15 m (width) × 16 m (height).

assumed on all sides of the detector (except the bottom) as well as between the top of the detector and the bottom of the roof. The roof is 3 m thick and assumed to be made of rock. The roof must be thick enough to remove the electromagnetic and hadronic component of atmospheric air showers.

Muons were sampled in ($\cos\theta$,E_μ)-plane from Eq. (1) at an altitude of 6 m (parallel with the top of the roof) over a surface area of 4×4 km^2 centered on the detector. Muons were propagated from their generation point to the detector using GEANT4; their point of first intersection with their detector as well as their momentum at that point were written to a text file so that truth information was preserved. A total of $2.8{\times}10^6$ muons with an average energy of about 10 GeV were recorded incident on the detector over 64.4 s of live-time giving an absolute atmospheric muon trigger rate of 44 kHz. It is interesting to note that of this 44 kHz, there is 19 Hz of upward-going muons due to scattering.

GEANT4 toolkit has been used to propagate the $2.8{\times}10^6$ muons discussed in the previous section through a liquid argon detector and electrons and positrons with a kinetic energy above 0.1 GeV have been recorded. An electron was recorded if:

- It had a neutral parent which was not a photon (e.g. a π^0).
- Its parent was a photon, but its grandparent was not an e^+ or e^- (we don't want to see every electron in an electromagnetic shower, just the first one).
- It had a neutral grandparent.

Since the muon interaction processes are random and the initial muon generation is extremely slow, each muon has been propagated approximately 10 times. Thus approximately 935.4 s of detector live time was simulated, resulting in 312,000 recorded electrons. This live time corresponds to 935.4/21053 = 0.0444 of a calendar year. Table 3 lists the processes that have been observed.

Table 3: The parents and grandparents of all the recorded electrons with energy above 0.1 GeV. No electrons due to kaons were observed.

GrandParent	Parent	Process	Number
μ	γ	$\mu \to \gamma \to e^+e^-$	282270
γ	e^+/e^-	electron scattering	26236
π^0	γ	$\pi \to \gamma\gamma \to e^+e^-$	3142
η	γ	η decay	62
η	π^0	η decay	1
$\eta\prime$	γ	$\eta\prime$ decay	19
γ	π^0	photonuclear resonance	20
γ	γ		4
γ	π^-	photonuclear resonance	1
π^-	π^0	pion decay	1
Σ^0	γ	Σ^0 decay	1
ρ^0	π^-	ρ^0 decay	1

As one can see from Table 3 the bulk of the recorded electrons originate from a bremsstrahlung photon (from the original muon), electron-electron scattering or neutral pion decay (photonuclear pion production). It is expected that these electrons should point back to the original muon track, or originate not too far off the muon track.

For each electron we calculated its point of closest approach (PoCA) to the original muon track as well as how far the vertex was away from the muon track. These variables are shown in Figure 10.

The PoCA technique is well known and should give reliable results, but the low-energy muons (which produce low-energy electrons) are deflected by multiple scattering and stochastic processes (in our case this is bremsstrahlung, for instance, leading to the production of an electron with energy greater than 0.1 GeV) inside the liquid argon. Thus the muon track is not simply a straight line. Figure 11 shows five example muon tracks which produced at least 1 electron with energy above 0.1 GeV. Assuming that the reconstruction software will be able to accurately reconstruct the muon track we have calculated the PoCA by tracking back the electron and comparing it to every point along the muon track (as recorded by G4Step). Similarly the distance variable is calculated by comparing the electron vertex to every point along the muon-track. The point of closest approach and the vertex-distance are plotted in Figure 12. The point of closest approach is by far much tighter than the distance variable, and will therefore be used in further analysis in this section.

Figure 13 shows distribution of the PoCA for electrons, the electron energy spectrum, and a scatter plot of PoCA versus energy. Not surprisingly the most energetic electrons point back closest to the track. Requiring that the point of closest approach be greater than 10 cm (i.e.

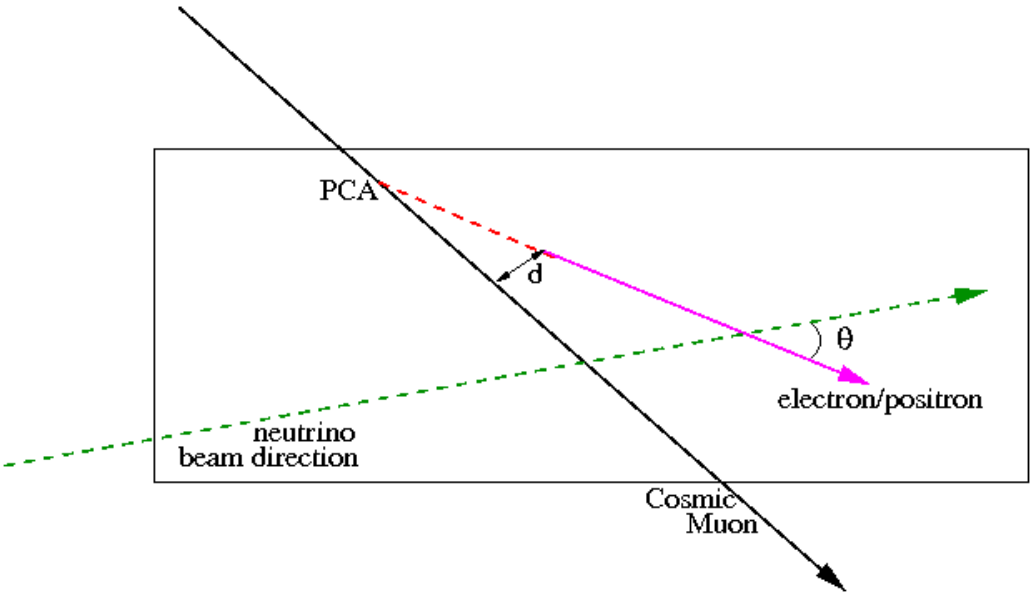

Figure 10: The vertex location and original momentum is used to determine how close the back-traced path of the electron gets to the muon track (PoCA). The distance variable shows how far the vertex is away from the muon track.

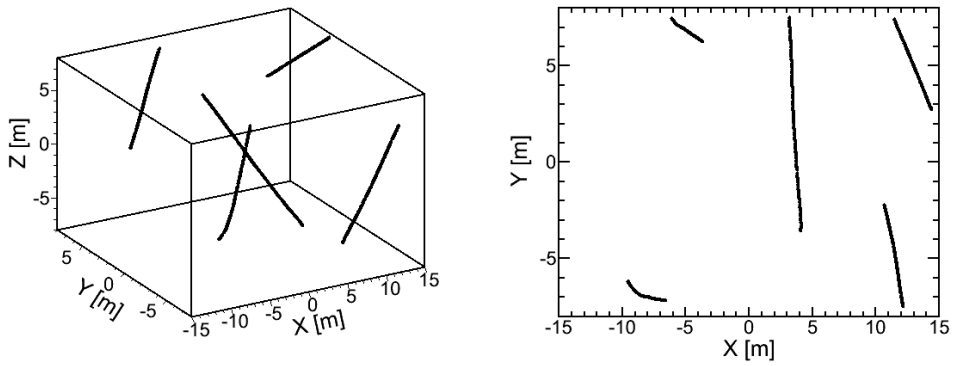

Figure 11: Five example muon tracks which have produced at least 1 electron with energy above 0.1 GeV. The left hand figure plots the 3-D track. The right figure plots the same tracks as viewed from the top of the detector. The effects of scattering are clearly visible.

problematic electrons) we see that the average electron energy drops dramatically. In fact the average electron energy, after the PoCA cut, is only 0.19 GeV. The neutrino energy of interest is 0.5 GeV to 5 GeV. Requiring that the electron energy be above 0.25 GeV greatly reduces the background and will have negligible effect on the oscillation analysis.

We have initially recorded 312,000 electron/positron events. By requiring that they have a PoCA greater than 10 cm and an energy above 0.25 GeV we are left with 38 electrons, more-

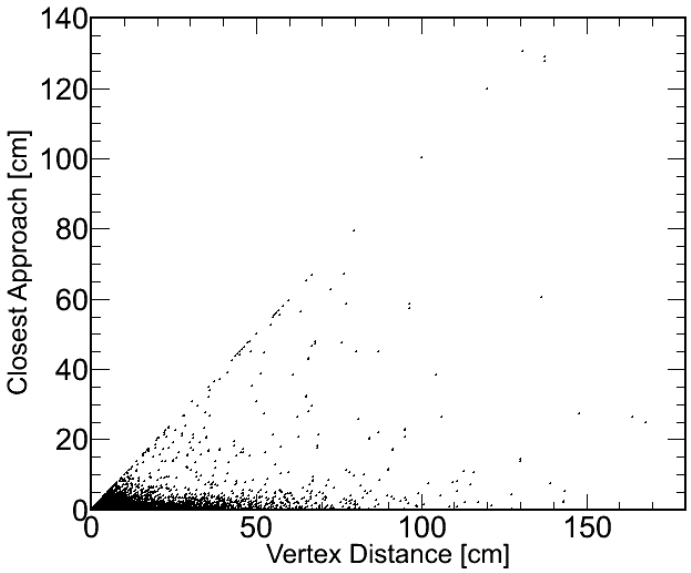

Figure 12: The point of closest of the electron track to the muon track versus the distance the electron vertex is to the muon track. The point of closest approach is always smaller than the vertex-distance.

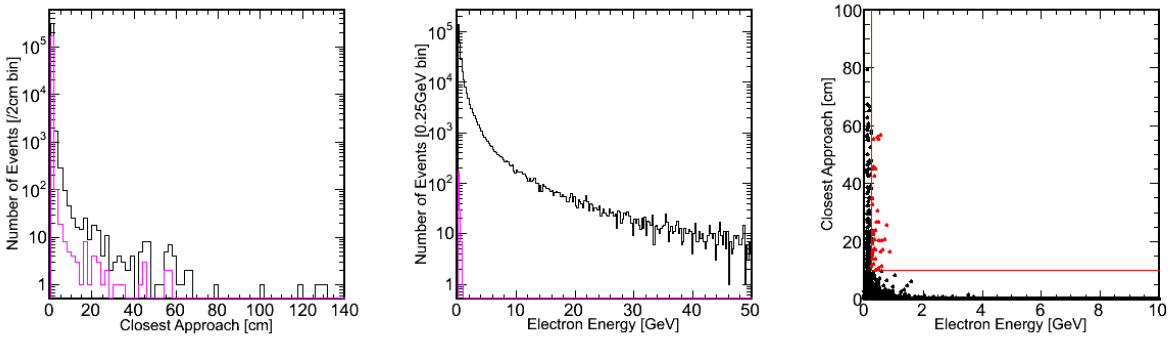

Figure 13: Left: the distribution of points of closest approach. The black histogram is for all electrons above 0.1 GeV, the magenta histogram is for electrons with energy above 0.25 GeV. Middle: electron energy spectrum. The black histogram is for all electrons, the magenta histogram is for all electrons with a PoCA greater than 10 cm. Right: the point of closest approach versus electron energy. The red data points are electrons that pass both selections: energy greater than 0.25 GeV and PoCA greater than 10 cm.

over these electrons originate from only 27 muons. Table 4 summarizes the selections and final electron event count.

Table 4: The number of electron/positron events remaining after selections.

Selection	Remaining Electrons	Events/year
Kinetic Energy >0.1 GeV	312208	7.03×10^6
PoCA>10 cm	207	4662
Electron Energy>0.25 GeV	38	856

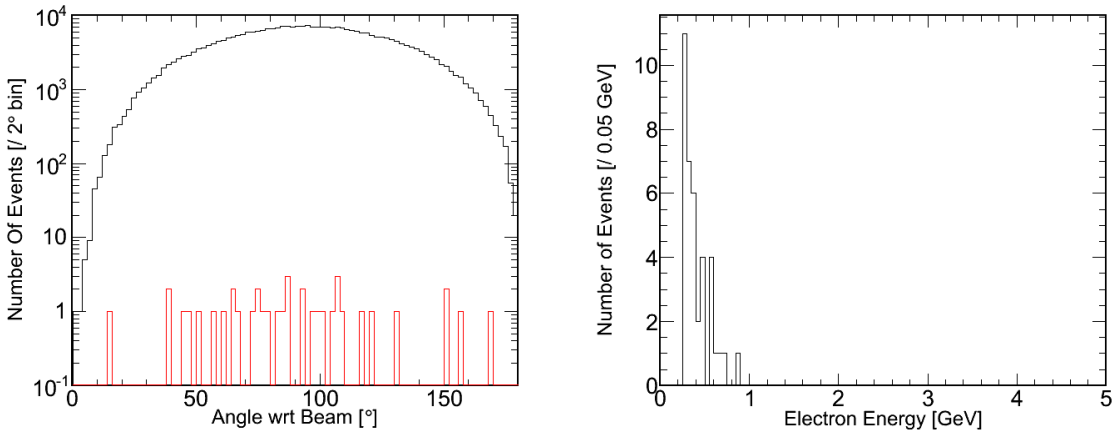

Figure 14: Left: the angular distribution of electrons with respect to the original neutrino direction (as defined in Figure 10. Very few events point back to the neutrino beam direction. Right: electron energy spectrum after selections. All electron events are below 1 GeV (in the second maxima of neutrino oscillations).

After these simple selections we are left with about 856 electrons per calendar year or 608 background electron events per year (in some cases 2 electrons belong to the same event). All 38 observed background electrons have originated from pion decay (which can be differentiated from ν_e charged current events at 98% efficiency. This would reduce the background to about 12 events/year. This number can be reduced even further if we require that the background electron be pointing in the roughly same direction as the neutrino beam (6° upwards). Figure 14 shows the angle of the electron with respect to the neutrino beam, before and after the discussed selections. Also shown in Figure 14 is the electron energy spectrum after the event selections.

Simulations show that bulk of the neutrino induced electron point to within 90° of the beam direction. It should be noted that the direction of the event, including both the hadronic and leptonic component, should strongly point back to the beam. Placing a directionality cut at 90° should therefore have very little effect on the neutrino-induced electrons but reduce the cosmogenic background by a factor of 2.

6 Background events without muon track in the detector

For muons that do not pass through the active detector, associated background events cannot be vetoed by connecting them to parent muons. These background events in the LAr detector are primarily induced by secondary neutral particles, such as neutrons, gamma-rays, π^0, etc. These neutral particles can produce charged particles in the detector with tracks that cannot be traced back to muons. While these background events have smaller rate compared to those produced by muons passing through the detector, they much more difficult to reject by kinematic cuts.

Fortunately, the reduction of this background can be done through a fiducial volume cut. The main focus of the simulations described in this section was to find the spatial distribution of the background events induced by muons that miss the detector and to determine the fiducial volume cut that will remove these events (see [16] for details).

A total of 10^{13} primary muons with energy $E_\mu > 10$ GeV have been generated on the surface of the Earth (10 km $\times$ 10 km) and transported to a LAr detector located 3 m below the ground. The total flux of muons through a horizontal surface at sea level was 100 m^{-2} s^{-1} for $E_\mu > 1$ GeV and 19.75 m^{-2} s^{-1} for $E_\mu > 10$ GeV. The statistics corresponded to 5063 s of live time or 5063/21053 = 0.240 of a calendar year (for 1.4 ms maximum drift time).

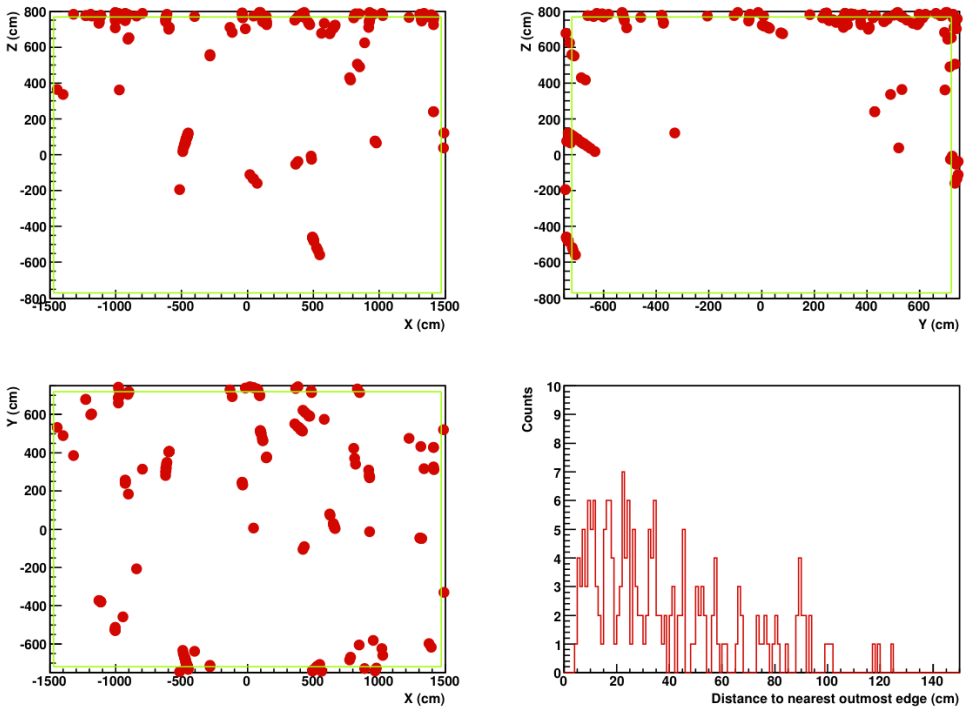

Figure 15: Positions of the first vertices of e^+/e^- with $E > 0.5$ GeV before the fiducial volume cut. All e^+e^- are produced by high-energy gamma-rays inside the LAr volume.

For beam-related physics, the region of interest lies between 0.5 GeV to 5 GeV. To reduce the CPU time for simulations, the event selection criteria have been imposed as follows:

1. All neutral particles (n, gamma-rays, π^0s, etc) with a kinetic energy greater than 0.5 GeV entering the LAr volume were recorded; once the particle kinetic energy drops below 0.5 GeV, the particle was 'killed'.

2. The first vertex of e^+e^--pair generated by a photon was recorded if this happened in LAr. Only particles with $E > 0.5$ GeV were recorded.

3. Since both e^+ and e^- are produced at the same vertex and started to ionize LAr immediately, the track reconstruction will identify this as a single event. If both e^+ and e^- have $E > 0.5$ GeV, one of them is removed to avoid double counting.

4. A fiducial cut was applied to remove particles from the 30 cm regions on the sides of the detector.

In 0.24 years of beam operation, 192 vertices (57 events) from gamma-ray induced pair production occurred in the detector before the fiducial cut or 798 vertices (237 events) per calendar year. (see Figure 15) while 96 vertices (22 events) remained after the fiducial cut (see Figure 16) or 400 vertices (92 events) per year.

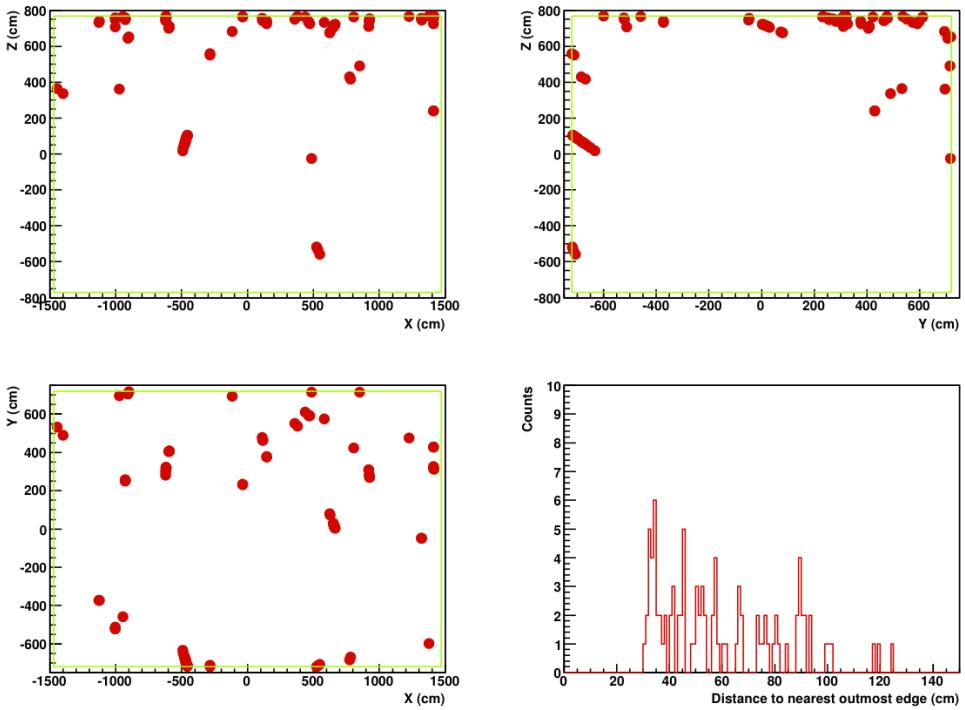

Figure 16: Positions of the first vertices of e^+e^--pairs with $E > 0.5$ GeV after the fiducial volume cut. All e^+/e^- are produced by high-energy gamma-rays inside the LAr volume.

Only a small fraction of events are leaking from the 30 cm thick volumes close to the detector surfaces. This indicates that the 30 cm fiducial volume cut seems to be reasonable.

With an additional rejection of 98% of events originating from photons rather than neutrinos [13], the number of background events will drop from 92 to about 2 per year. Thus we conclude that events from near-miss muons will not be a problem given the nominal fiducial volume cuts and e/γ separation efficiency.

Additional background will come from muons which cross dead regions of the detector and hence will be missed. Due to a small aperture for these muons (small volume of dead regions) their rate should not be high and the current design includes a 30 cm fiducial volume cut around the inner dead spaces.

7 Attenuation of muon flux with depth

Of course, background events caused by muons can be suppressed, if necessary, by positioning an LBNE detector underground in a shallow depth cavern. The attenuation of the muon flux through a sphere is given in Table 5. Figure 17 shows the muon flux through the LAr detector as a function of depth.

Table 5: Total muon flux (no energy cut) through a sphere and its attenuation for different shallow depth locations assuming flat surface and rock density of 2.71 g/cm^3.

Depth, m w. e.	0	10.2	20	50	100	150	200
Depth, m	0	3.764	7.380	18.45	36.90	55.35	73.80
Muon flux, cm^{-2} s^{-1}	2.07×10^{-2}	1.14×10^{-2}	6.50×10^{-3}	1.99×10^{-3}	6.02×10^{-4}	2.71×10^{-4}	1.47×10^{-4}
Attenuation factor	1	1.82	3.18	10.4	34.4	76.7	141
Muon flux at $\theta > 70°$ $\phi < 20°$, cm^{-2} s^{-1}	1.02×10^{-4}	5.88×10^{-5}	3.39×10^{-5}	1.02×10^{-5}	2.92×10^{-6}	1.23×10^{-6}	6.21×10^{-7}
Attenuation factor for selected muons	1	1.74	3.02	10.0	35.0	83	164

8 Conclusions

Two independent techniques have been investigated to reduce muon-associated backgrounds using the ability of the LAr detector to reconstruct muon tracks and electron showers and separate electron- from gamma-induced showers. Both techniques have been shown to be viable, even without the assumption of a photon trigger system or fast timing veto.

For background events with associated muons crossing the LAr volume, rejecting all electromagnetic cascades with angles with respect to the muon track smaller than 10° and distances from muons smaller than 50 cm will reduce the background event rate at 0.5-5 GeV to about 1500 events per calendar year (after additional assumption that photon events can be correctly identified as such in 98% of cases). Additional selection of candidate signal events to be within 40° from the beam direction reduces the background to about 150 events per calendar year.

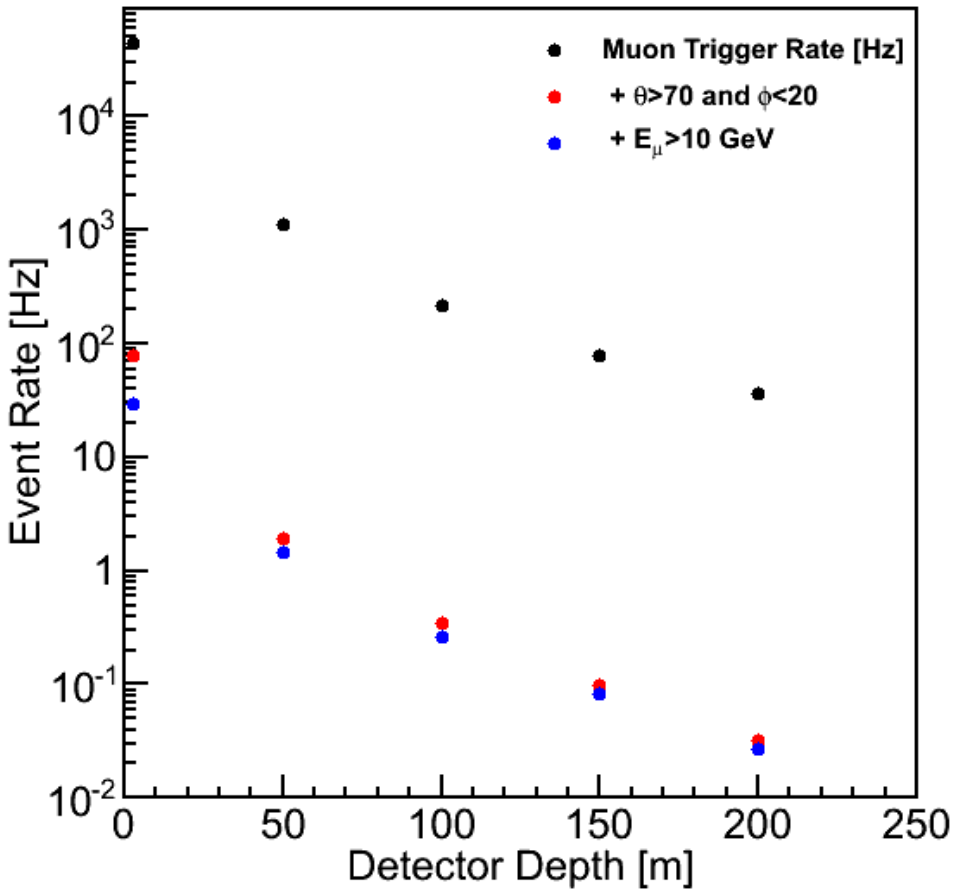

Figure 17: Muon flux through the LAr detector as a function of depth. The red points indicate the rate for near horizontal muons within twenty azimuthal degrees of the beam direction. The blue points are horizontal muons with energy > 10 GeV.

A powerful technique using calculation of the point of closest approach of the electromagnetic cascade to nearby muons, if applied alone, will reduce background events by more than 3 orders of magnitude down to about 600 events per calendar year. With an efficient e/γ discrimination the background rate will be reduced down to about 12 events/year. This technique can be applied together with other cuts. Since the cuts on the angle, distance and PoCA are not independent, it is not clear at the moment what the reduction will be if all cuts discussed here are applied together. This is currently under study.

There is a significant number of K_L^0 produced but first simulations indicate that less than 200 of them can decay into electrons with energies greater than 0.1 GeV in a calendar year (no such event is detected but statistics is small). Since the decays are almost all at rest, the electron energies tend to be highly peaked at energies < 0.25 GeV. This is currently the most uncertain muon-induced background, but it can be reliably studied by increasing statistics.

Positioning a LAr detector behind a hill will help to suppress the background events caused by near horizontal muons moving close to the neutrino beam direction. If background events can be rejected based on their angle with respect to the beam direction, then removing near horizontal muons parallel to the beam using additional rock shielding and applying the cut on the angle w.r.t. the beam θ_b for signal events, may reduce the background by a significant factor. This factor depends on the exact location of the detector with respect to the hill and full Monte Carlo is required to calculate it. This rejection will certainly be efficient for signal events with energy greater than 1-2 GeV concentrated within 40° w.r.t. the beam.

For background events with no muon passing through the detector, the suggested fiducial volume cut of 30 cm from the surfaces looks adequate after rejecting 98% of remaining events as photon-induced cascades rather than neutrino-induced cascades.

Finally, muon-induced backgrounds can be measured to a very high precision by looking at events occuring during random, beam-off times. Thus any small remaining backgrounds will have very little uncertainly associated with them and can be statistically subtracted.

References

[1] T. K. Gaisser. Cosmic Rays and Particle Physics (Cambridge University Press, 1990).

[2] J. De Jong. LBNE-doc-3144 (December 2010).

[3] J. De Jong. LBNE-doc-6150 (July 2012); private communication (2012).

[4] V. A. Kudryavtsev. Muon simulations for LBNE using MUSIC and MUSUN, LBNE-doc-5833 (April 2012).

[5] D. Chirkin. Preprint arXiv:hep-ph/0407078v1 (2004).

[6] Particle Data Group. Review of Particle Physics, *Phys. Rev. D* **66** (2002) 010001.

[7] L. Goodenough et al. Cosmic Ray Backgrounds in the LBNE Far Detector, LBNE-doc-5958 (May 2012).

[8] D. Gerstle and S. Pordes. Cosmic Ray Rates on the Surface for a Liquid Argon TPC, LBNE-doc-5950 (August 2006).

[9] V. A. Kudryavtsev. Cosmogenic Background for Beam Neutrinos at the Surface: Some Thoughts, LBNE-doc-5973 (May 2012).

[10] S. Zeller and M. Bishai. Private communications (2012).

[11] E. Church. Private communications (2012).

[12] V. A. Kudryavtsev et al. Muon-induced background for beam neutrinos on the surface, LBNE-doc-6159 (July 2012).

[13] A Proposal for a Detector 2 km Away from the T2K Neutrino Source (2005).

[14] M. Diwan. Private communication (2012).

[15] J. De Jong. Background estimations for a surface detector, LBNE-doc-6150 (July 2012).

[16] C. Zhang et al. A part of cosmic-ray induced background study for the LBNE beam related physics, LBNE-doc-6164 (July 2012).